ASDJ
AINSHAMS DENTAL JOURNAL

Print ISSN 1110-7642
Online ISSN 2735-5039

AIN SHAMS DENTAL JOURNAL
Official Publication of Ain Shams Dental School
september2022 • Vol. 27

Involvement of Vascular Endothelial Growth Factor in Deferoxamine Radioprotection of Rat Oral Mucosa

Maryam Salah Ibrahim[1], Dahlia Ghazy Mohamed Rateb[2], Rania Ahmed Awwad[3]

Aim: The purpose of this study was to explore the potential of DFO an iron chelator drug in prevention of irradiation-induced oral mucositis and to monitor the immune-expression of vascular endothelial growth factor (VEGF) in irradiated and radioprotected rats.
Materials & Methods: Thirty male Albino rats were divided into three groups (n =10): Control group (GC): received no treatment, Irradiated group (GI): received a single radiation dose of 10 Gray on the head and neck region, Deferoxamine group (GD): rats received intraperitoneal injection of 50 mg/kg of Deferoxamine for three days before being irradiated like in GI. Rats were sacrificed the 12th day post-irradiation. Their tongues were dissected and processed for H&E staining and immunohistochemical detection of VEGF, the angiogenic marker.
Results: Examination of GI revealed an apparent reduction in the thickness of the epithelium and some ulcerative areas. In the lamina propria, dilated engorged blood vessels and degenerative areas were detected. GI showed VEGF immunopositivity in the epithelial layers as well as in the endothelial and connective tissue cells of the lamina propria. VEGF immunopositivity was statistically reduced when compared with GC. GD showed an apparent increase in the epithelium thickness with restoration of epithelial integrity and minimal degeneration of the lamina propria. GD presented marked VEGF immunostaining with a statistically significant increase compared to GI.
Conclusion: The findings of this study showed that Deferoxamine exerted a protective effect against radiation-induced oral mucositis with possible association of VEGF overexpression in reduction of mucositis histopathological damage.

Keywords: Deferoxamine, irradiation, mucositis, ventral surface of tongue, VEGF

1. Teaching assistant at Oral Biology department, Faculty of Dentistry, Fayoum University, Egypt.
2. Associate Professor of Oral Biology Faculty of Dentistry, Ain Shams University, Egypt.
3. Associate Professor of Oral Biology, Faculty of Dentistry, Ain Shams University and head of histopathology department, Faculty of Dentistry, O6U, Egypt.
Corresponding author: Maryam Salah Ibrahim, email: msio2@fayoum.edu.eg

Introduction

Radiotherapy remains the cornerstone in treatment of patients with head and neck cancers, but it is unfortunately accompanied by inevitable damage to oral mucosa and surrounding structures in the radiation field [1,2]. Oral mucositis (OM), being one of the major complications secondary to cancer therapy was reported to occur in up to 100% of patients undergoing radiation therapy for head and neck [3]. OM refers to erythema and/or ulceration of the oral mucosa, it is a painful condition that causes dysphagia, reduce oral intake, weight loss and secondary infections. Eventually, severe complications lead to cancer treatment interruption, extend hospitalization and the use of feeding tubes which could worsen tumor prognosis and increase health care cost [4-6]. Hence, adequate prevention and timely management of radiation induced-OM is crucial in limiting the severity of mucositis and improving compliance to radiation for better tumor control [7].

Following irradiation (IR), injury of basal epithelial cells, vascular endothelial and submucosal cells initiate OM [8,9]. By interacting with biological tissues, ionizing radiation produces reactive oxygen species (ROS) that damage proteins, DNA and lipids causing cell dysfunction and apoptotic cell death [10]. Vascular endothelial cell damage following IR was previously detected in vitro [11-13] and also in various organs of different animals [14-18]. In the oral cavity, injury of capillary endothelial cells with reduced vascular density of murine salivary glands was detected four hours after IR [13]. More importantly, the transfer of vascular endothelial growth factor (VEGF) complementary DNA to glands endothelial cells could overcame IR drawbacks by increasing angiogenesis and restoring the salivary fluid secretion.

Deferoxamine (DFO) is an FDA approved iron chelator used to treat conditions of acute iron poisoning and chronic iron overload in patients who undergo multiple blood transfusions [19,20]. It has also shown antioxidant and antiapoptotic [21-25] as well as angiogenic [26-28] and wound healing properties [29]. DFO was also proposed as a therapeutic agent that could improve tissue repair and regeneration in irradiated mice's' salivary glands [22] and ameliorate radiation-induced skin injury [30,31,32].

However, the radioprotective efficacy of DFO was not thoroughly investigated, therefore, this study was designed to investigate the protective potential of DFO on radiation-induced oral mucositis in rats' tongue. The angiogenic effect of DFO pretreatment was immunohistochemically investigated through expression of VEGF antibody.

Materials and Methods

Experimental Animals and Ethical Statement

This study was conducted on thirty male Albino rats, weighing about 200-250 grams each. Rats were housed in separate cages in Ain Shams University Animal House under controlled temperature, humidity, and dark-light cycle. Rats were maintained under good ventilation and adequate stable diet comprising of fresh vegetables, dry bread and tap water for the duration of the experiment. The whole experiment was conducted as reviewed and approved by institution guidelines of Ain Shams University Ethical Committee (Approval number: FDASU – REC IR011744).

Experimental Design

The rats were randomly divided into three groups (n =10): (1) *Control group:* received no treatment or irradiation (2) *Irradiation group (GI):* exposed to a single dose of 10 Gray (Gy) radiation to the head and neck

region (3) *DFO pretreated group (GD):* rats were intraperitoneally injected with 50 mg/kg body weight DFO for three consecutive days before irradiation with 10 Gy to head and neck region. All animals were sacrificed at the 12th day following irradiation exposure.

Administration of DFO

Sterile lyophilized Deferoxamine methylate powder supplied in glass vials (500 mg) Desferal ™ (Novartis Pharma, USA) was dissolved in 40 ml of sterilized water to be injected intraperitoneally at a dose of 50 mg/kg body weight for three consecutive days before irradiation [22].

Animals Irradiation

Rats of GI and GD were immobilized by anesthesia protocol, they were injected intraperitoneally with sodium pentobarbital (Nembutal®, 40 mg/kg body weight) and ketamine chloride (Ketalar®, 40 mg/kg body weight) [33]. Anaesthetized rats were irradiated at the National Cancer Institute (NCI), a cobalt 60 source (energy 1.25 MV, THERATRON 780 E) was used at a dose rate of about 139cGy/min. Heads of 10 rats were positioned in the same irradiation field for radiation exposure at a single dose of 10 Gy and the rest of the body was covered with a lead plate [34,35].

Specimen Preparation

All animals were sacrificed by anesthetic overdose 12 days after irradiation, their tongues were dissected to a sample size of five mm in diameter, fixed in 10% neutral buffered formalin, dehydrated in graded alcohol, cleared in xylene and then embedded in paraffin. Sections of 4–6 µ thickness of the ventral surface of the tongue were cut and processed for light microscopic examination of hematoxylin and eosin (H&E) staining and anti-VEGF immunohistochemical staining.

Immunohistochemistry

- Four-micron thick sections were fixed for an hour in a 65º C oven. - Slides were placed in a coplin jar filled with 60 ml of Triology working solution, the jar was securely positioned in the autoclave at a temperature of 120 C^0 for 15 min after which pressure was released and the coplin jar was removed to let the slides cool for 30 min. - Sections were then washed and soaked in Tris Buffer Saline (TBS) to adjust the pH, this was repeated between each step of the technique. - Sections were incubated in 0.05 mg/ml proteinase K in 0.05 M Tris-HCl, 0.01 M EDTA, and 0.01 M NaCl, pH 7.8, for 10 minutes at 37°C to allow nuclear permeation.

-Quenching endogenous peroxidase activity was performed by immersing slides in 3% hydrogen peroxide for 10 minutes. Abroad spectrum LAB-SA detection system from Invitrogen (Sigma Pharmaceuticals) was used to detect any antigen-antibody reaction in the tissues. - Background staining was blocked by placing 2-3 drops of 10% non-immune goat serum blocker on each slide and incubating for 10 min in a humidity chamber. - Excess serum was drained from each slide, 2-3 drops of ready to use primary mouse monoclonal anti-VEGF were added and slides were then incubated for one hour in the humidity chamber.

-Biotinylated secondary antibody was then applied to each slide for 20 minutes followed by a 20-minute incubation with the enzyme conjugate.

- DAB chromogen was prepared, and 2-3 drops were applied on each slide for two minutes and then rinsed, followed by Mayer Hematoxylin counterstaining application. -All the slides were examined under a light microscope for evidence of a brown reaction product of the DAB substrate.

Histomorphometric Measurements

Histological and immunohistochemical assessments were performed to respectively measure the epithelial thickness in H&E sections and area percentage (%) of VEGF immunopositivity in immunohistochemical sections. This was carried out in the Precision

Measurement Unit, Oral Pathology Department, Faculty of Dentistry, Ain Shams University using Image J software (Version 1.41a, NIH, USA).

The thickness of the epithelium covering the ventral surface of the tongue was assessed in H&E-stained sections using Leica Quin 500 analyzer computer system by drawing a straight line demonstrating the distance from the basement membrane to the top layer of epithelial cells. Thickness was estimated at four different points, in four different fields of view for each specimen, under magnification (×200). The image analyzer is calibrated automatically to convert the measurement units (pixels) produced by the image analyzer program into actual micrometer units.

For evaluation of VEGF immunopositivity, four microscopic fields showing highest immunopositivity were assessed for each section. The area % of immuno-positively stained area was measured automatically, it was expressed as a percentage the immuno-positively area to the total area of the microscopic field. Fields were recorded with a digital camera (Canon DSLR EOS 1200D, Japan) attached to a light microscope (BX60, Olympus, Japan). The obtained images were then transferred to the computer system for analysis.

Statistical analysis

Recorded data were analyzed using the statistical package for social sciences, version 20.0 (SPSS Inc., Chicago, Illinois, USA). Quantitative data were expressed as mean± standard deviation (SD). As the data followed normal distribution, the one-way analysis of variance (ANOVA) was used when comparing between means of the variables (epithelial thickness and area fraction % of VEGF immune-staining) in the different groups, followed by least significant difference (LSD) post hoc test if result of (ANOVA) test was significant. *P* value of ≤0.05 was considered statistically significant and P-value <0.001 was considered as highly significant.

Results

i. Histological Results

Control Group (GC)

Examination of histological sections of the rat's ventral surface of tongue in GC showed normal architecture of epithelium, lamina propria and striated muscles. The epithelial covering consisted of a keratinized stratified squamous epithelium. The epithelial layer was separated from the underlying lamina propria by the basement membrane (BM) which presented short and numerous epithelial ridges. The lamina propria (LP) presented connective tissues cells, fibers and blood vessels (BVs) (Fig 1a).

Irradiated group (GI)

Histological examination of this group revealed apparent reduction in the thickness of both, the epithelium and its overlying keratin layer which also showed separation from underlying layer (Fig1b, e). The epithelial ridges appeared reduced in height and nuclear changes (Fig 1d) were detected in the basal cells (Fig 1b). Focal discontinuity of epithelium and BM was also detected (Fig 1c).

The underlying LP showed degenerative areas (Fig 1c, d), many BVs were dilated and engorged with RBCs (Fig 1b, d), others showed fibrotic vessel wall (Fig 1e). The LP revealed areas of heavy chronic inflammatory cell infiltration (Fig 1d) whereas extensive areas of degeneration and hyalinization were noticed in the LP of some sections (Fig 1e). Areas of separation were seen between lingual muscle fibers (Fig 1b, c).

Group pretreated with DFO (GD)

This group showed a histological picture of epithelium, LP and muscle fibers almost comparable to control. An apparent increase in epithelial thickness and overlying keratin layer was observed when compared to

irradiated group and epithelial ridges appeared more defined. Many small BVs were observed in the LP and some degenerated areas were seen between lingual muscle fibers (Fig 1f).

ii. Immunohistochemical staining results (Anti VEGF Antibody)

Control Group (GC)

Examination of anti-VEGF stained sections of the rat's lingual ventral surface of GC revealed well expressed immunopositivity in the basal, prickle and granular epithelial cell layers. The immunoreaction was mainly cytoplasmic with nuclear involvement. VEGF immune-expression was seen in the endothelium lining BVs of the LP and to a less extent in LP cells where immunoreaction was mainly cytoplasmic with some cells displaying nuclear involvement (Fig 2a).

Irradiated Group (GI)

Examination of GI showed weak VEGF immunopositivity in the epithelium and LP. Almost all epithelial layers displayed cytoplasmic immunopositivity, nuclear involvement was mainly detected in basal cell layer. Endothelial and connective cells of the LP displayed cytoplasmic immunostaining with only few nuclei involved (Fig 2b).

DFO pretreated group (GD)

The ventral mucosa of rat's tongues of GD showed generalized marked VEGF immunostaining. Positive immunostaining was detected in all epithelial layers with nuclear involvement in basal and spinous cell layers as well as in LP cells and BVs endothelia (Fig 2c).

iii. Statistical Analysis

1. Area percentage of vascular endothelial growth factor immunohistochemical expression

By using ANOVA, a highly significant difference between means of the three studied groups was found (p-value <0.001). By using post hoc LSD test, GI showed a significantly reduced VEGF area % immunopositivity compared with GC and GD. Meanwhile, VEGF area % in GD was significantly higher compared with GI and GC (table 1, fig.3).

2. Epithelial thickness

By using ANOVA, there was highly statistically significant difference between the three studied groups (p-value <0.001). By using post hoc LSD test, the epithelial thickness of GI was significantly reduced compared with GC and GD. Meanwhile GD showed a significant increase compared with GI and a significant decrease in the epithelial thickness when compared with GC (table 2, fig.4).

Discussion

The effective concrete intervention for prevention and/or treatment of radiation-induced OM has not been yet identified and only palliative measures were reported [36]. The ideal strategies that could restrain the severity of collateral radiation-induced damage are either prophylactic treatment modalities or those targeting the earliest stages of OM [30]. In a previous rat model of radiotherapy-induced glossitis, endothelial cell injury and apoptosis were reported as early as three days after IR, representing an early sign of OM which preceded epithelial injury [37]. Therefore, this study explored the potential of DFO, the iron chelator drug with angiogenic properties [26-28] in preventing radiation-induced oral mucositis.

In this study, the ventral surface of the tongue was the tissue of choice to explore the effect of IR on oral mucosa due to its greater sensitivity to ionizing radiation as it does not present a thick keratinized layer, it can also provide sufficient space for adequate tissue collection [38]. Moreover, tongue ulceration was described to represent mucosal damage occurring in high-grade OM in patients undergoing cancer treatment [39].

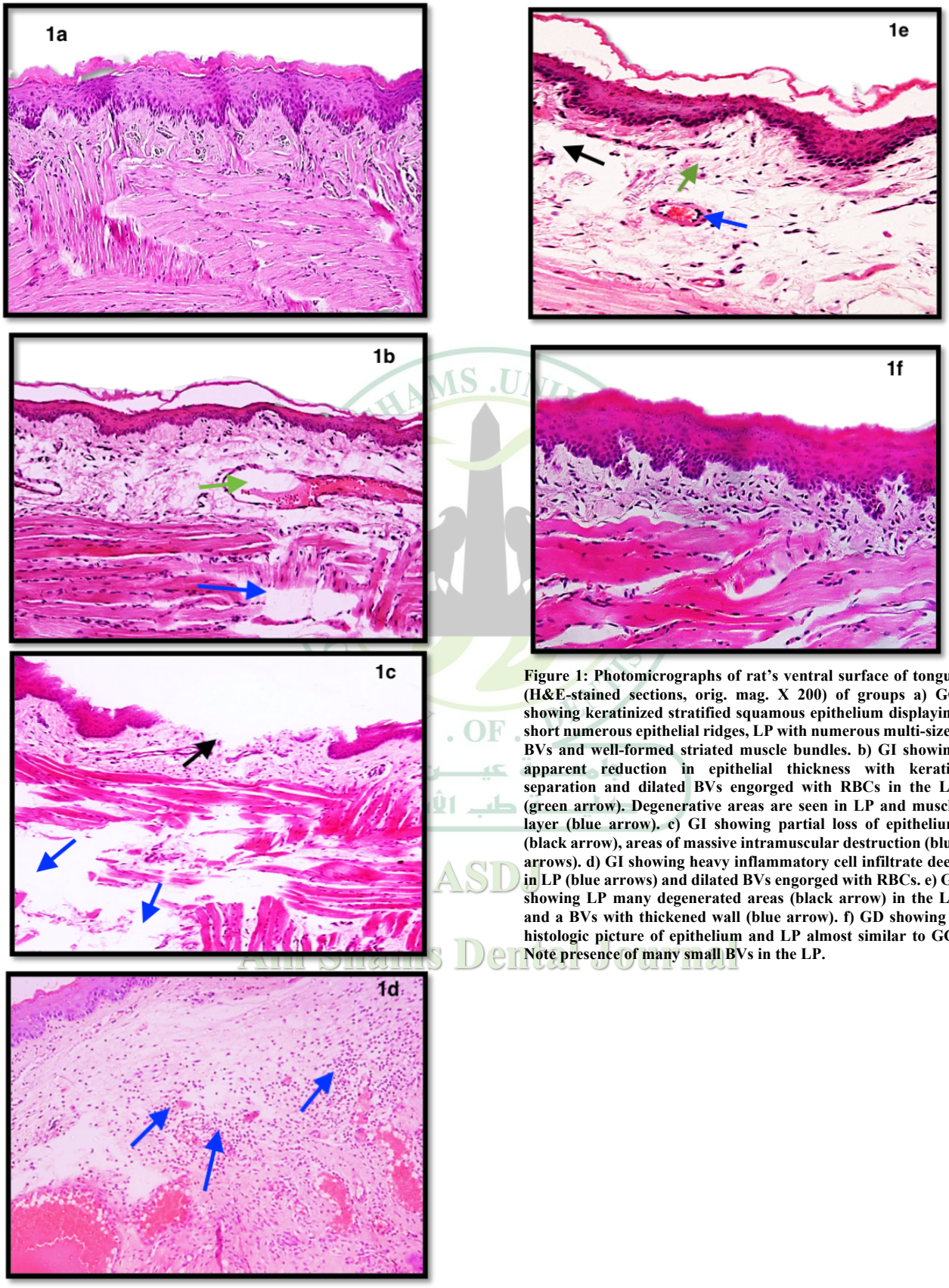

Figure 1: Photomicrographs of rat's ventral surface of tongue (H&E-stained sections, orig. mag. X 200) of groups a) GC showing keratinized stratified squamous epithelium displaying short numerous epithelial ridges, LP with numerous multi-sized BVs and well-formed striated muscle bundles. b) GI showing apparent reduction in epithelial thickness with keratin separation and dilated BVs engorged with RBCs in the LP (green arrow). Degenerative areas are seen in LP and muscle layer (blue arrow). c) GI showing partial loss of epithelium (black arrow), areas of massive intramuscular destruction (blue arrows). d) GI showing heavy inflammatory cell infiltrate deep in LP (blue arrows) and dilated BVs engorged with RBCs. e) GI showing LP many degenerated areas (black arrow) in the LP and a BVs with thickened wall (blue arrow). f) GD showing a histologic picture of epithelium and LP almost similar to GC. Note presence of many small BVs in the LP.

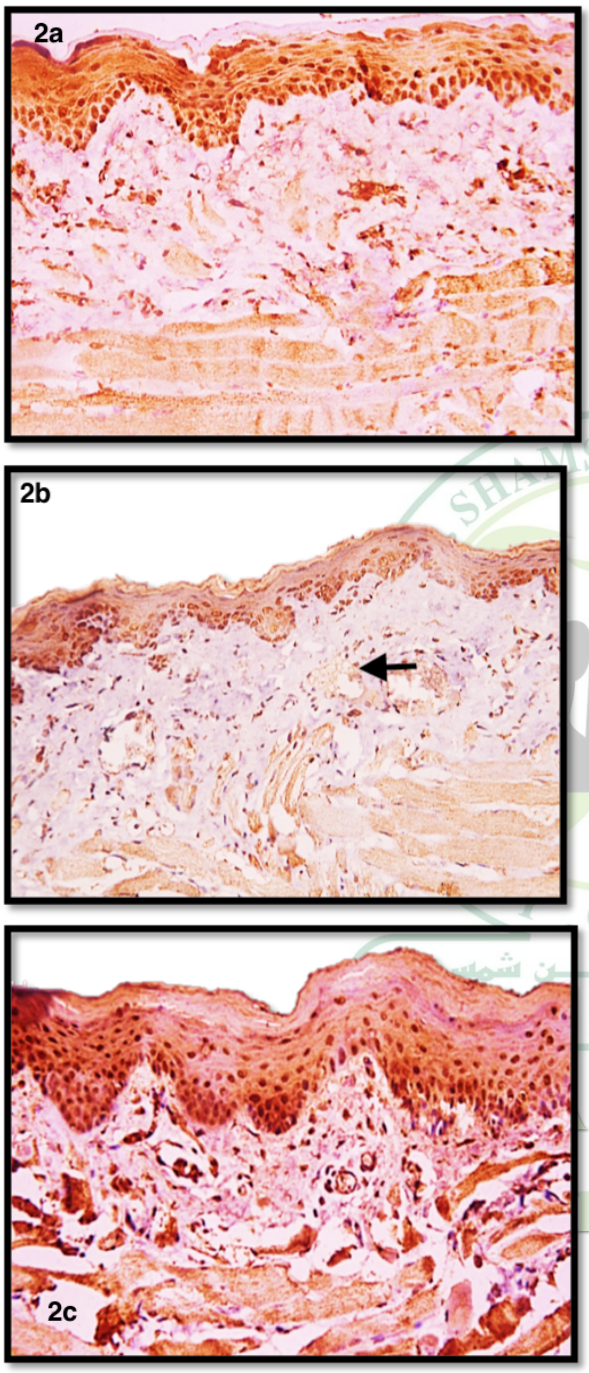

Figure 2: Photomicrographs of VEGF immunolabelling of ventral surface of rat's tongue (Anti VEGF X400): a) GC displays well expressed VEGF immuno-reactivity in basal, prickle and granular epithelial cell layers as well as many BVs and cells of LP. b) GI showing weak VEGF immune reaction in the epithelium and in BVs and cells of LP (black arrow). c) GD showing marked VEGF immunostaining in the epithelium, LP cells and BVs endothelia.

Table 1: Comparison between groups GC, GI and GD according to means of area percentage of VEGF immunopositivity

Area %	GC	GI	GD	ANOVA	p-value
Mean± SD	19.55±0.57B	12.77±5.29C	23.68±2.01A	25.325	<0.001**
Range	19.15-20.21	8.21-18.56	21.41-25.24		

**p-value <0.001 highly significant
Different capital letters indicate significant difference at (p<0.05) between means

Table 2: Comparison between means of epithelial thickness in groups GC, GI and GD

Mean Epithelial Thickness	GC	GI	GD	ANOVA	p-value
Mean± SD	716.18±216.06A	122.18±34.75C	444.46±26.57B	49.128	<0.001*
Range	542.73-958.21	100.12-162.24	417.78-470.93		

**p-value <0.001 highly significant
Different capital letters indicate significant difference at (p<0.05) between means

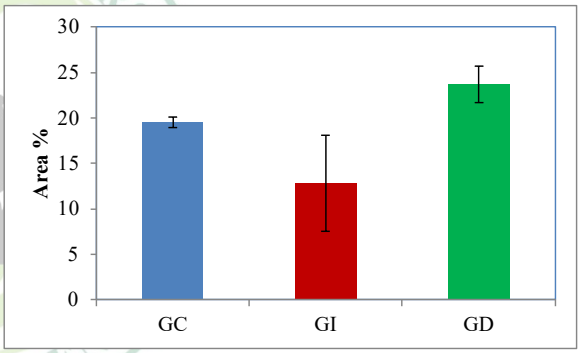

Fig. 3: Bar chart showing means of area percentage of VEGF immunopositivity in groups GC, GI and GD

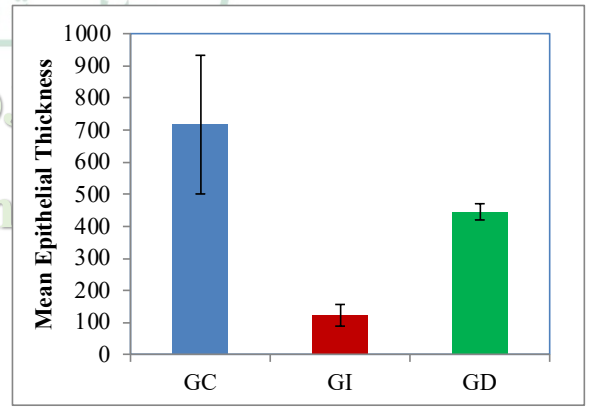

Fig. 4: Bar chart showing means of epithelial thickness in groups GC, GI and GD

In the current study, the route of DFO administration was chosen to be the intraperitoneal route as it was reported to be a well-tolerated route in conditions of head and neck IR associated with oral soft tissue atrophy [40]. The sacrificing date was chosen to be the 12th day following IR based on rat model of radiation-induced glossitis where histopathological changes developed at 5to 6 day post-irradiation and aggravated from 7th to15th day [41].

When H&E stained sections of the irradiated group were examined, an apparent reduction in the thickness of the lingual epithelium was observed, when compared with GC. Ulcerative lesions were also evident. Nuclear changes were detected in the basal cells and epithelial ridges appeared reduced in height. In the underlying LP, many BVs were dilated, engorged with RBCs and others showed thickened vessel wall. Heavy chronic inflammatory cell infiltration and degenerative areas were also detected.

Histopathologic findings of GI are in accordance with study on radiation-induced glossitis rat model where development of ulcerative lesions, appearance of extensive engorged BVs and inflammatory cells were reported at 7-15 days post-irradiation [41].

In irradiated oral mucosa, the reduction in epithelial thickness is attributed to interference of ionizing radiation with cell mitosis. This reduces the regenerative capacity of the oral mucosa and causes a steady decline in the number of epithelial cells. It was further clarified that epithelium was affected by apoptotic and cytotoxic effects of IR on the dividing basal cells within the first week of IR [8]. The reduction in epithelial thickness detected in GI is in agreement with earlier findings of radiation-induced OM studies [33, 42] in the lingual epithelia of rats and mice respectively.

In the current study, the reduced epithelial thickness observed in H&E sections of GI was found to be statistically significant when compared with GC. This finding is parallel with results of a study [38] reporting a decrease in epithelial cell density of human mucosal biopsies taken before and during head and neck radiotherapy course. The decrease was about 50% of the pre-irradiation value during the first week following IR. The ulcerative lesions observed in H&E stained sections were similarly reported in previous studies of radiotherapy-induced glossitis [37,43,44]. Oral ulcer development was reported to occur after the first week of IR, when epithelial cell death threshold was exceeded and desquamating cells reached the basement membrane which then disrupted exposing the underlying LP [9, 45].

It is understood that IR initiates injury-producing pathways that affect epithelial and endothelial cells through activation of nuclear factor-κB and NRF-2 that stimulated the production of pro-inflammatory mediators such as tumour necrosis factor (TNF-α), and interleukins (IL1and IL6). Continuous expression of these inflammatory mediators prolonged tissue damage, resulting in the loss of oral membrane integrity and development of oral ulcers [46,47].

In the current study, presence of nuclear changes specially in the basal epithelial cells of the irradiated group come in agreement with the results of a study reporting clumped chromatin, nuclear swelling and pleomorphism in upon irradiation [48]. Radiation-induced mucositis was reported to be triggered by direct damage to basal epithelial cells and underlying cells. DNA fragmentation is known to be the primary effect of ionizing radiation causing cell damage, while reactive oxygen species generation mediates non-DNA damage [9].

In the present study, vascular changes were detected in the LP of the irradiated

group. Mechanisms underlying vascular injury following IR were clarified in several studies and were mainly attributed to augmented expression of TNFα and platelet-derived growth factor (PDGF) [49] which stimulate events including intimal thickening with concomitant shrinkage in lumen size and break down of elastic and muscle fibers of the vessel walls eventually leading to functional inefficiency of the BVs [9, 50]. The early decrease in perfusion following IR was also reported to occur when leukocytes infiltrate BVs and fibrin plugs form [30]. Moreover, the endothelial cells lining the BVs swell and undergo hyperplasia leading to small vessel occlusion, hypoperfusion and eventual tissue hypoxia [31,48]. Finally, it was postulated that following IR, ROS caused damage to the endothelial cells lining the local BVs in the surrounding healthy tissues [51].

In a previous study [9], the vascular changes occurring in OM were described to be accompanied by edema of epithelial rete pegs which go along with our results. Meanwhile, destruction of BVs integrity and vasodilatation observed in irradiated group of this study are in parallel with those reported in a earlier study of radiation-induced glossitis [37].

The degenerative areas detected in the LP of GI are in accordance with an earlier study finding [52]. Inflammation and ROS generation following IR were explained to cause oxidative stress to cellular components leading to activation of matrix metalloproteases (MMPs) causing subsequent extracellular damage [53].

In the current study, the inflammatory cell infiltration detected in the LP of irradiated rats was similarly reported to accompany mucositis ulcer [8]. It was reported to result from bacterial cell wall products that reached the submucosa and stimulated macrophages proinflammatory cytokines production and release of additional MMPs resulting in more inflammation. Our results are also in agreement with findings reporting inflammatory cell infiltration in the lingual ventral surface of head and neck irradiated rats, two weeks following IR [34].

Examination of H&E stained sections of rats pretreated with DFO revealed an improved histological picture with increased small BVs when compared with irradiated group. The histological observations of GD parallel those found in earlier DFO studies [30, 31,54] reporting that prophylactic administration of DFO was found to reduce injury to ischemic skin tissues. The association of DFO in upregulating cytokines and growth factors following IR are thought to be mediated by mainly two main mechanisms depending on its iron chelating properties [31,55]: Firstly, DFO stabilizes hypoxia-inducible factor -1 alpha (HIF-1α), the powerful transcription factor for numerous proangiogenic genes by limiting iron-dependent degradation. This consequently upregulates the downstream of pro-angiogenic growth factors production like VEGF and endothelial nitric oxide synthase [55 -57] improving tissue vascularization and augmenting oxygen and nutrient supply to injured tissue. Secondly, DFO decreases oxidative stress and inflammation accompanying tissue ischemia by restraining iron-mediated ROS generation [58,59]. DFO was therefore found to possess a crucial advantage over other drugs which increase HIF-1α levels [29]. Interestingly, histological sections of the current study showed that DFO pretreated group was more similar to control than irradiated group by most measures. This could highlight a promising approach to address detrimental collateral oral mucosal injury following head and neck IR.

To evaluate whether vascular alterations detected in H&E sections of the present study resulted from variation in

VEGF expression, its immune-expression was examined in the different groups. VEGF is established as a key regulator of physiological angiogenesis during development and also in pathology [60].

In the current study, the control mucosa revealed positive VEGF immunostaining in many epithelial, endothelial as well as connective tissue cells, which is in accordance with previous reported results in rat's tongue [61]. Although VEGF acts mostly on endothelial cells, it was also reported to bind to VEGF receptors on hematopoietic stem cells and monocytes of the connective tissue [62]. Meanwhile, keratinocytic VEGF was shown to be a potent and selective mitogen for dermal microvascular endothelial cells during physiological processes such as skin wound repair [63].

In the current study, examination of VEGF immunolabelled sections of GI revealed an apparent decrease in VEGF immune-expression when compared with GC. This was statistically supported by the significant area % reduction of VEGF immunolabelling when comparing GI with GC. Reduced VEGF immune-expression in GI could be explained based on the findings reporting apoptosis of vascular endothelial cells in radiotherapy-induced glossitis rat model and clarifying that the highest percentage of apoptosis was detected at eight days post-irradiation [37]. Results of GI go along with those reporting that only irradiation dose higher than 10 GY could produce VEGF in human vascular endothelial cells [64].

In the present work, immunohistochemical examination of VEGF expression in the tongue mucosa of the DFO pretreated group showed a marked immunopositivity in epithelial, CT and endothelial cells. This was statistically supported by the significantly higher VEGF area% immunolabelling of GD when compared to control and irradiation groups.

In several studies, DFO was reported to promote revascularization of ischemic tissues in various pathologic conditions via VEGF- mediated pathway [26, 32, 65-67]. It was explained that in hypoxic conditions, expression of HIF-1α (the oxygen-sensitive molecule) is upregulated with subsequent regulation of target genes like VEGF. Normally, HIF-1α is degraded by prolyl hydroxylase domain-containing protein 2 (PHD2). Through its iron chelating property, DFO could stabilize HIF-1α by chelation of the iron co-factor for PHD2 activity [66]. This lead to increase generation of angiogenic factors, including VEGF and recruitment of endothelial progenitor cells enhancing blood vessels formation [24,68,69].

DFO was previously described to possess a dual nature that promoted BV growth [70], as it could prevent endothelial cell death by reducing perivascular ROS and additionally, depending on its angiogenic property, it could also increase microvascular regeneration. So, this DFO dual nature could explain the significant increase of VEGF area % immunopositivity in GD compared with the other two studied groups and precisely with GC, where mean of VEGF area % immunopositivity in GD was found to surpass that of the control.

In the present study, the significant increase in area % of VEGF immunopositivity in GD when compared with GI suggested enhanced angiogenesis in the DFO pretreated group. This was revealed histologically by appearance of numerous small BVs and could be also correlated with the minimal histopathologic damage revealed in GD. This suggestion is based on the clarification of Hou's study [65] when investigating the effects of DFO intraperitoneal injection on cutaneous wound. The investigators explained that DFO enhanced vasculature formation, increased

blood circulation near the affected site bringing nutrients, factors and cytokines that helped restore damaged tissue.

In conclusion, this study suggested that DFO pretreatment could mitigate the deleterious effects of irradiation on oral mucosa, offering a potential treatment modality for its protection from radiation-induced mucositis. Upregulation of VEGF immune-expression could be involved in DFO radioprotection which also raise the possibility of oral mucosa radioprotection by manipulating VEGF expression. Further investigations using different DFO doses, duration and routes of delivery are required to get its optimum radioprotective beneficial effect.

References

1. Sroussi HY, Epstein JB, Bensadoun RJ, Saunders DP, Lalla RV, Migliorati CA, Heaivilin N, Zumsteg ZS. Common oral complications of head and neck cancer radiation therapy: mucositis, infections, saliva change, fibrosis, sensory dysfunctions, dental caries, periodontal disease, and osteoradionecrosis. Cancer Med. 2017 Dec;6(12):2918-31.
2. Basile D, Di Nardo P, Corvaja C, Garattini SK, Pelizzari G, Lisanti C, Bortot L, Da Ros L, Bartoletti M, Borghi M, Gerratana L, Lombardi D, Puglisi F. Mucosal injury during anti-cancer treatment: from pathobiology to bedside. Cancers (Basel). 2019 Jun 20;11(6):857.
3. Lalla RV, Bowen J, Barasch A, Elting L, Epstein J, Keefe DM, McGuire DB, Migliorati C, Nicolatou-Galitis O, Peterson DE, Raber-Durlacher JE, Sonis ST, Elad S; Mucositis Guidelines Leadership Group of the Multinational Association of Supportive Care in Cancer and International Society of Oral Oncology (MASCC/ISOO). MASCC/ISOO clinical practice guidelines for the management of mucositis secondary to cancer therapy. Cancer. 2014;120(10):1453-61.
4. Pico JL, Avila-Garavito A, Naccache P. Mucositis: Its occurrence, consequences, and treatment in the oncology setting. Oncologist. 1998;3(6):446-51.
5. Peterson DE, Keefe DM, Hutchins RD, Schubert MM. Alimentary tract mucositis in cancer patients: impact of terminology and assessment on research and clinical practice. Support Care Cancer. 2006;14(6):499-504.
6. Elting LS, Cooksley CD, Chambers MS, Garden AS. Risk, outcomes, and costs of radiation-induced oral mucositis among patients with head-and-neck malignancies. Int J Radiat Oncol Biol Phys. 2007; 68 (4):1110-20.
7. Mallick S, Benson R, Rath GK. Radiation induced oral mucositis: a review of current literature on prevention and management. Eur Arch Otorhinolaryngol. 2016; 273(9):2285-93.
8. Sonis ST, Elting LS, Keefe D, Peterson DE, Schubert M, Hauer-Jensen M, Bekele BN, Raber-Durlacher J, Donnelly JP, Rubenstein EB; Mucositis Study Section of the Multinational Association for Supportive Care in Cancer; International Society for Oral Oncology. Perspectives on cancer therapy-induced mucosal injury: pathogenesis, measurement, epidemiology, and consequences for patients. Cancer. 2004;100(9 Suppl):1995-2025.
9. Ps SK, Balan A, Sankar A, Bose T. Radiation induced oral mucositis. Indian J Palliat Care. 2009;15(2):95-102.
10. Redza-Dutordoir M, Averill-Bates DA. Activation of apoptosis signalling pathways by reactive oxygen species. Biochim Biophys Acta. 2016;1863(12):2977-2992.
11. Zhou Q, Zhao Y, Li P, Bai X, Ruan C. Thrombomodulin as a marker of radiation-induced endothelial cell injury. Radiat Res. 1992;131(3):285-9.
12. Mao XW. A quantitative study of the effects of ionizing radiation on endothelial cells and capillary-like network formation. Technol Cancer Res Treat. 2006;5(2):127-34.
13. Sugumaran P, Narayanan V, Zhu D, Medhora M, Jacobs ER, Chandramohan Y, Selvaraj V, Dhanasekaran A. Prophylactic supplementation of 20-HETE ameliorates hypoxia/reoxygenation injury in pulmonary vascular endothelial cells by inhibiting apoptosis. Acta Histochem. 2020;122 (1) :151461.
14. Peña LA, Fuks Z, Kolesnick RN. Radiation-induced apoptosis of endothelial cells in the murine central nervous system: protection by fibroblast growth factor and sphingomyelinase deficiency. Cancer Res. 2000;60(2):321-7.
15. Paris F, Fuks Z, Kang A, Capodieci P, Juan G, Ehleiter D, Haimovitz-Friedman A, Cordon-Cardo C, Kolesnick R. Endothelial apoptosis as the primary lesion initiating intestinal radiation damage in mice. Science. 2001;293(5528):293-7.
16. Cotrim AP, Sowers A, Mitchell JB, Baum BJ. Prevention of irradiation-induced salivary hypofunction by microvessel protection in mouse salivary glands. Mol Ther. 2007;15(12):2101-6.
17. Rannou E, François A, Toullec A, Guipaud O, Buard V, Tarlet G, Mintet E, Jaillet C, Iruela-Arispe ML, Benderitter M, Sabourin JC, Milliat F. In vivo evidence for an endothelium-dependent mechanism in radiation-induced normal tissue injury. Sci Rep. 2015; 5: 15738.

18. Venkatesulu BP, Mahadevan LS, Aliru ML, Yang X, Bodd MH, Singh PK, Yusuf SW, Abe JI, Krishnan S. Radiation-induced endothelial vascular injury: a review of possible mechanisms. JACC Basic Transl Sci. 2018;3(4):563-572.
19. Banner W Jr, Tong TG. Iron poisoning. Pediatr Clin North Am. 1986;33(2):393-409.
20. Ackrill P, Day JP. The use of Desferrioximine in dialysis-associated aluminium disease. Contrib Nephrol. 1993; 102:125-34.
21.Arent CO, Réus GZ, Abelaira HM, Ribeiro KF, Steckert AV, Mina F, Dal-Pizzol F, Quevedo J. Synergist effects of n-acetylcysteine and deferoxamine treatment on behavioral and oxidative parameters induced by chronic mild stress in rats. Neurochem Int. 2012;61(7):1072-80.
22. Zhang J, Cui L, Xu M, Zheng Y. Restoring the secretory function of irradiation-damaged salivary gland by administrating deferoxamine in mice. PLoS One. 2014; 9(11): e113721.
23. Codd R, Richardson-Sanchez T, Telfer TJ, Gotsbacher MP. Advances in the chemical biology of Desferrioxamine B. ACS Chem Biol. 2018;13(1):11-25.
24. Holden P, Nair LS. Deferoxamine: an angiogenic and antioxidant molecule for tissue regeneration. Tissue Eng Part B Rev. 2019;25(6):461-70.
25. G Paradellis D, D Panousopoulos GS, G Mathioulaki A, E Papalois A, N Nomikos T, Theocharis S, A Gkiokas G, F Arkadopoulos N. Antioxidant preconditioning attenuates liver ischemia/reperfusion injury after hepatectomy in swine. J BUON. 2021;26(3):1159-64.
26. Ikeda Y, Tajima S, Yoshida S, Yamano N, Kihira Y, Ishizawa K, Aihara K, Tomita S, Tsuchiya K, Tamaki T. Deferoxamine promotes angiogenesis via the activation of vascular endothelial cell function. Atherosclerosis. 2011;215(2):339-47.
27. Efird WM, Fletcher AG, Draeger RW, Spang JT, Dahners LE, Weinhold PS. Deferoxamine-soaked suture improves angiogenesis and repair potential after acute injury of the chicken achilles tendon. Orthop J Sports Med. 2018;6(10) :2325967118802792.
28. Farzan R, Moeinian M, Abdollahi A, Jahangard-Rafsanjani Z, Alipour A, Ebrahimi M, Khorasani G. Effects of amniotic membrane extract and Deferoxamine on angiogenesis in wound healing: an in vivo model. J Wound Care. 2018;27(Sup6): S26-S32.
29. Tchanque-Fossuo CN, Dahle SE, Buchman SR, Isseroff RR. Deferoxamine: potential novel topical therapeutic for chronic wounds. Br J Dermatol. 2017;176(4) :1056-59.
30. Shen AH, Borrelli MR, Adem S, Deleon NMD, Patel RA, Mascharak S, Yen SJ, Sun BY, Taylor WL 4th, Januszyk M, Nguyen DH, Momeni A, Gurtner GC, Longaker MT, Wan DC. Prophylactic treatment with transdermal Deferoxamine mitigates radiation-induced skin fibrosis. Sci Rep. 2020;10(1):12346.
31. Lavin CV, Abbas DB, Fahy EJ, Lee DK, Griffin M, Diaz Deleon NM, Mascharak S, Chen K, Momeni A, Gurtner GC, Longaker MT, Wan DC. A comparative analysis of Deferoxamine treatment modalities for dermal radiation-induced fibrosis. J Cell Mol Med. 2021;25(21) :10028-38.
32. Tevlin R, Longaker MT, Wan DC. Deferoxamine to minimize fibrosis during radiation therapy. Adv Wound Care (New Rochelle). 2022; 11(10):548-59.
33. Elsaadany B, El Kholy S, El Rouby D, Rashed L, Shouman T. Effect of transplantation of bone marrow derived mesenchymal stem cells and platelets rich plasma on experimental model of radiation induced oral mucosal injury in albino rats. Int J Dent. 2017; 2017: 8634540.
34. Aboushady, IM, Mubarak, R.T, El-mougy, SA, Rashed, LA and El-desouky, A. The effect of transplanted bone marrow stem cells on the tongue of irradiated rats (Histological and Immunohistochemical study). J Am Sci. 2012; 8(11), 553–61.
35. Miyamoto H, Kanayama T, Horii K, Kawai T, Tsuchimochi T, Shigetomi T, Shibamoto Y, Shibuya Y. The relationship between the severity of radiation-induced oral mucositis and the myeloperoxidase levels in rats. Oral Surg Oral Med Oral Pathol Oral Radiol. 2015;120(3):329-36.
36. Daugėlaitė G, Užkuraitytė K, Jagelavičienė E, Filipauskas A. Prevention and treatment of chemotherapy and radiotherapy induced oral mucositis. Medicina (Kaunas). 2019;55(2):25.
37. Li CY, Hong Y, Tao XA, Xia J, Cheng B. The correlation between the severity of radiotherapy-induced glossitis and endothelial cell injury in local tissues in a rat model. Med Oral Patol Oral Cir Bucal. 2011;16(6):e711-5.
38. Dörr W, Hamilton CS, Boyd T, Reed B, Denham JW. Radiation-induced changes in cellularity and proliferation in human oral mucosa. Int J Radiat Oncol Biol Phys. 2002; 52(4):911-7.
39. Sciubba JJ, Goldenberg D. Oral complications of radiotherapy. Lancet Oncol. 2006;7(2):175-83.
40. Flacco J, Chung N, Blackshear CP, Irizarry D, Momeni A, Lee GK, Nguyen D, Gurtner GC, Longaker MT, Wan DC. Deferoxamine preconditioning of irradiated tissue improves perfusion and fat graft retention. Plast Reconstr Surg. 2018;141(3):655-65.
41. Li CY, Chen XH, Tao XA, Xia J, Cheng B. The development and inflammatory features of radiotherapy-induced glossitis in rats. Med Oral Patol Oral Cir Bucal. 2011; 16(3): e348-53.

42. Zhao J, Kim KA, De Vera J, Palencia S, Wagle M, Abo A. R-Spondin1 protects mice from chemotherapy or radiation-induced oral mucositis through the canonical Wnt/beta-catenin pathway. Proc Natl Acad Sci U S A. 2009;106(7):2331-6.
43. Dörr W, Kummermehr J. Proliferation kinetics of mouse tongue epithelium under normal conditions and following single dose irradiation. Virchows Arch B Cell Pathol Incl Mol Pathol. 1991;60(5):287-94.
44. Zhu J, Zhang H, Li J, Zheng X, Jia X, Xie Q, Zheng L, Zhou X, Wang Y, Xu X. LiCl promotes recovery of radiation-induced oral mucositis and dysgeusia. J Dent Res. 2021;100(7):754-63.
45. Redding SW. Cancer therapy-related oral mucositis. J Dent Educ. 2005; 69(8) :919-29.
46. Scully C, Sonis S, Diz PD. Oral mucositis. Oral Dis. 2006; 12(3):229-41
47. Logan RM, Gibson RJ, Sonis ST, Keefe DM. Nuclear factor-κappa B (NF-kappa B) and cyclooxygenase-2 (COX-2) expression in the oral mucosa following cancer chemotherapy. *Oral Oncol.* 2007;43: 395–401.
48. Sheaff M, Baithun S. Pathological effects of ionizing radiation. Curr Diagn Pathol.1997; 4 (2): 106-115.
49. Silverman S Jr, Shillitoe EJ. Etiology and predisposing factors. In: Silverman S Jr, ed. Oral cancer. 4th ed. Atlanta, GA: American Cancer Society. 1998: 7-24.
50. Bentzen SM. Preventing or reducing late side effects of radiation therapy: radiobiology meets molecular pathology. Nat Rev Cancer. 2006;6(9):702-13.
51. Mittal M, Siddiqui MR, Tran K, Reddy SP, Malik AB. Reactive oxygen species in inflammation and tissue injury. Antioxid Redox Signal. 2014; 20(7):1126-67.
52. Shih A, Miaskowski C, Dodd MJ, Stotts NA, MacPhail L. Mechanisms for radiation-induced oral mucositis and the consequences. Cancer Nurs. 2003;26(3):222-9.
53. Pillai S, Oresajo C, Hayward J. Ultraviolet radiation and skin aging: roles of reactive oxygen species, inflammation and protease activation, and strategies for prevention of inflammation-induced matrix degradation - a review. Int J Cosmet Sci. 2005;27(1):17-34.

54. Duscher D, Neofytou E, Wong VW, Maan ZN, Rennert RC, Inayathullah M, Januszyk M, Rodrigues M, Malkovskiy AV, Whitmore AJ, Walmsley GG, Galvez MG, Whittam AJ, Brownlee M, Rajadas J, Gurtner GC. Transdermal deferoxamine prevents pressure-induced diabetic ulcers. Proc Natl Acad Sci U S A. 2015;112(1):94-9.
55. Lintel H, Abbas DB, Lavin CV, Griffin M, Guo JL, Guardino N, Churukian A, Gurtner GC, Momeni A, Longaker MT, Wan DC. Transdermal deferoxamine administration improves excisional wound healing in chronically irradiated murine skin. J Transl Med. 2022;20(1):274.
56. Bianchi L, Tacchini L, Cairo G. HIF-1-mediated activation of transferrin receptor gene transcription by iron chelation. Nucleic Acids Res. 1999;27(21):4223-7.
57. Shen X, Wan C, Ramaswamy G, Mavalli M, Wang Y, Duvall CL, Deng LF, Guldberg RE, Eberhart A, Clemens TL, Gilbert SR. Prolyl hydroxylase inhibitors increase neoangiogenesis and callus formation following femur fracture in mice. J Orthop Res. 2009;27(10):1298-305.
58. Thomas C, Mackey MM, Diaz AA, Cox DP. Hydroxyl radical is produced via the Fenton reaction in submitochondrial particles under oxidative stress: implications for diseases associated with iron accumulation. Redox Rep. 2009;14(3):102-8.
59. Chang HC, Wu R, Shang M, Sato T, Chen C, Shapiro JS, Liu T, Thakur A, Sawicki KT, Prasad SV, Ardehali H. Reduction in mitochondrial iron alleviates cardiac damage during injury. EMBO Mol Med. 2016;8(3):247-67.
60. Ferrara N, Davis-Smyth T. The biology of vascular endothelial growth factor. Endocr Rev. 1997;18(1):4-25.
61. Maejima, M., Maruoka, Y., Sawada, T., Ando, T., Kobayashi, M., and Ogiuchi, H. Expression of vascular Endothelial Growth Factor (VEGF) and specific receptors (Flt-1 and Flk-1) in rat tongue Carcinogenesis Induced by 4-Nitroquinoline 1-Oxide. Acta Histochemica et Cytochemica. 2002; 35(4): 331-41.
62. Ferrara N, Gerber HP, LeCouter J. The biology of VEGF and its receptors. Nat Med. 2003;9(6):669-76.
63. Wilgus TA, Matthies AM, Radek KA, Dovi JV, Burns AL, Shankar R, DiPietro LA. Novel function for vascular endothelial growth factor receptor-1 on epidermal keratinocytes. Am J Pathol. 2005;167(5):1257-66.
64. Kim EJ, Lee H, Lee YJ, Sonn JK, Lim YB. Ionizing radiation regulates vascular endothelial growth factor-a transcription in cultured human vascular endothelial cells via the PERK/eIF2α/ATF4 Pathway. Int J Radiat Oncol Biol Phys. 2020;107(3):563-570.
65. Hou Z, Nie C, Si Z, Ma Y. Deferoxamine enhances neovascularization and accelerates wound healing in diabetic rats via the accumulation of hypoxia-inducible factor-1α. Diabetes Res Clin Pract. 2013;101(1): 62-71.
66. Wang C, Cai Y, Zhang Y, Xiong Z, Li G, Cui L. Local injection of deferoxamine improves

neovascularization in ischemic diabetic random flap by increasing HIF-1α and VEGF expression. PLoS One. 2014; 9(6):e100818.
67. Mehrabani M, Najafi M, Kamarul T, Mansouri K, Iranpour M, Nematollahi MH, Ghazi-Khansari M, Sharifi AM. Deferoxamine preconditioning to restore impaired HIF-1α-mediated angiogenic mechanisms in adipose-derived stem cells from STZ-induced type 1 diabetic rats. Cell Prolif. 2015;48(5):532-49.
68. Chang EI, Loh SA, Ceradini DJ, Chang EI, Lin SE, Bastidas N, Aarabi S, Chan DA, Freedman ML, Giaccia AJ, Gurtner GC. Age decreases endothelial progenitor cell recruitment through decreases in hypoxia-inducible factor 1alpha stabilization during ischemia. Circulation. 2007; 116(24): 2818-29.
69. Weng R, Li Q, Li H, Yang M, Sheng L. Mimic hypoxia improves angiogenesis in ischaemic random flaps. J Plast Reconstr Aesthet Surg. 2010; 63(12): 2152-9.
70. Jiang X, Malkovskiy AV, Tian W, Sung YK, Sun W, Hsu JL, Manickam S, Wagh D, Joubert LM, Semenza GL, Rajadas J, Nicolls MR. Promotion of airway anastomotic microvascular regeneration and alleviation of airway ischemia by deferoxamine nanoparticles. Biomaterials. 2014;35(2):803-13.